Kinetic model of ethylene oxidation by *p*-benzoquinone in solutions of cationic palladium(II) complexes in a binary acetonitrile—water solvent*

G. E. Efremov, E. A. Bovyrina, E. A. Katsman, R. S. Shamsiev, and O. N. Temkin★

MIREA — Russian Technological University (M. V. Lomonosov Institute of Fine Chemical Technologies), 86 prosp. Vernadskogo, 119571 Moscow, Russian Federation.
E-mail: olegtemkin@mail.ru

A kinetic model was developed for the reaction of ethylene oxidation to acetaldehyde by *p*-benzoquinone (Q) at 30 °C catalyzed by the cationic palladium(II) complexes in a binary acetonitrile—water solvent at a molar fraction of water of 0.67. The three-route mechanism was proposed that adequately describes all experimental dependences of the concentrations of consumed ethylene on time at various partial ethylene pressures and concentrations of palladium, perchloric acid, and Q. The time-dependent (a) palladium distribution between the intermediates and (b) ratio of the rates of steps of acetaldehyde oxidation *via* different routes were analyzed. The role of the Pd^{II}, Pd^{I}, and Pd^{0} complexes in the catalytic formation of olefins was discussed. The quantum chemical estimates of the composition of the coordination sphere for several intermediates and probabilities of some elementary steps in the reaction mechanism were obtained.

Key words: kinetic model, oxidation, ethylene, *p*-benzoquinone, palladium, cationic complexes, acetonitrile, quantum chemical modeling.

The participation of the cationic Pd^{II} complexes in nonaqueous and acidic water-organic media in catalysis has attracted research interest long ago.[1—12] Among the reactions involved is the oxidation of olefins.[5—12] The study of the kinetics of cyclohexene oxidation by *p*-benzoquinone (Q)[9] and measurements of kinetic isotope effects (KIE) in the reactions of ethylene and cyclohexene oxidation[11] in acetonitrile (AN)—H_2O/D_2O systems made it possible to elucidate the main features of the mechanism of these reactions. The mechanism includes the addition of a water molecule to the π-complexes at the slow step without preliminary dissociation, the formation of the cationic Pd^{I} complexes (Pd_2Q^{2+}) during cyclohexene oxidation, and four routes for the reaction of cyclohexanone formation.[11] As a result of the determination of the initial rates, the kinetics[13] of dec-1-ene oxidation by oxygen in solutions of the $PdCl_2$ complex with (−)sparteine (diazatetracycloheptadecane) as a ligand in a dimethyl acetamide (DMA)—water system at 70 °C and 1.7 atm O_2 was described. The data obtained also brought some light on the reactivity of the cationic palladium complexes, since two chloride ions are replaced by water or DMA and the dicationic π-complex is formed in the reaction medium. When the water concentration changed up to 8 mol L^{-1}, it was found[13] that the reaction rate can be described by the third-order equation with respect to $[H_2O]_\Sigma$. An intermediate containing the dicationic π-complex with three water molecules was proposed[13] to explain this fact, although the structure of this complex is a transition state rather than an intermediate. Since the system contains no acid, the KIE equal to 1.6—2.6 observed[11] in the H_2O/D_2O system can be related to both the reversible deprotonation of the product of water molecule addition to the cationic π-complex and hydrolysis of Pd^{2+}. In an AN—water system, the dependences of the oxidation rates of cyclohexene[9,10] and ethylene[14] by *p*-benzoquinone on the molar fraction of water are described by curves with two maxima[9,10] or one maximum.[14] The maximum on the curve describing the initial rates of ethylene oxidation by *p*-benzoquinone approximately corresponds to the composition of the associate $AN/H_2O = 2$ (MeCN...H—O—H...NCMe).

The kinetic model of ethylene oxidation to acetaldehyde in a $Pd(OAc)_2$—$HClO_4$—$LiClO_4$—Q—AN—H_2O system has recently been constructed[15] using the results of measuring the initial rates (R_0) of ethylene consumption taking into account the lack of KIE in AN—H_2O/D_2O (see Ref. 11) and C_2H_4/C_2D_4 (see Ref. 12) systems. The

* Dedicated to one of the founders of modern catalysis by metal complexes, Academician of the Russian Academy of Sciences I. I. Moiseev on the occasion of his 90th birthday. Both the discovery of the reaction of olefin oxidation with the formation of carbonyl compounds and vinyl and alkenyl esters catalyzed by the palladium complexes and also the development of the coordination and organometallic chemistry of palladium are associated with the name of I. I. Moiseev.

Published in Russian in *Izvestiya Akademii Nauk. Seriya Khimicheskaya,* No. 7, pp. 1366—1375, July, 2019.

dependences $R_0 = f(P(C_2H_4)$ or $[H^+])$ are described by the "saturation" curves, *i.e.*, curves with a limit of function increasing, $R_0 = k[Pd]_\Sigma$, and $R_0 = f([Q])$ is extremal with a maximum near $[Q] = 0.1$ mol L^{-1}. The kinetic equation experimentally verified at constant concentrations of water and acetonitrile contains the second-order polynomial with respect to $[H_2O]$ in the numerator and the third-order polynomial with respect to $[H_2O]$ in the denominator. No quantitative analysis of this dependence was performed, because the reaction rate also depends on the acetonitrile concentration under the conditions of a significant change in the properties of the binary water—AN solvent. Since the process of ethylene (and cyclohexene) oxidation in a closed system is characterized by the kinetic curve with two regions: fast and slow,[9,11,12,15] it seemed of interest to develop a kinetic model that describes the process up to high degrees of *p*-benzoquinone consumption. This model could be helpful in revealing the nature of these two regions and details of the mechanism related to the possibility of the Pd^I complexes to participate in the process of ethylene oxidation.

Experimental

The procedure of a kinetic experiment was earlier described in detail.[11,12,15] The selectivity to acetaldehyde is ≥95%. The quantum chemical calculations were performed using the PRIRODA program.[16,17] The scalar relativistic approximation of the DFT-PBE density functional method[18] combined with the L11 full-electron basis set was used.[19] The solvent effect was taken into account by the addition of several molecules of water and acetonitrile. For the steps involved the cationic palladium complexes, the influence of the counterion was evaluated by the addition of ClO_4^- anions solvated by water molecules, *i.e.*, influence of the formation of ion pairs.

The kinetic curves used for the construction of the kinetic model of the process are presented in Figs 1—4 for various concentrations of Pd^{II}, $HClO_4$, Q, and C_2H_4 ($P(C_2H_4)$). The inverse problem of chemical kinetics (estimation of the rate constants of the kinetic model) was solved using the program package.[20] The initial rate constants were estimated taking into account the rate values of the quasi-stationary process in the initial region[15] and in the slow regions of the kinetic curves.

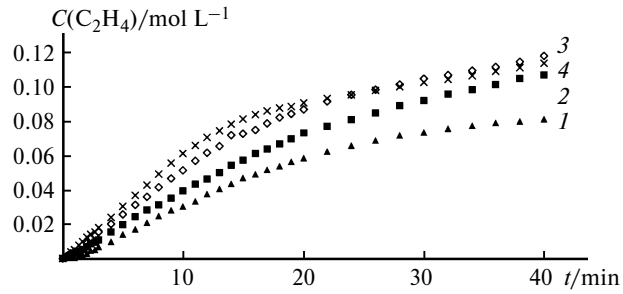

Fig. 1. Time dependences of the concentration of consumed ethylene at various partial pressures of ethylene: $P(C_2H_4) = 0.23$ (*1*), 0.42 (*2*), 0.6 (*3*), and 0.83 atm (*4*); $[Pd]_\Sigma = 0.0005$ mol L^{-1}, $[Q] = 0.2$ mol L^{-1}, $[HClO_4] = 0.2$ mol L^{-1}, $\alpha(H_2O) = 0.67$ molar fractions.

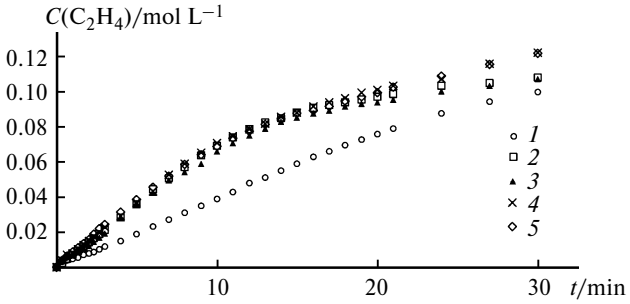

Fig. 2. Time dependences of the consumed ethylene concentration at various acid concentrations: $[HClO_4] = 0.1$ (*1*), 0.2 (*2*), 0.3 (*3*), 0.4 (*4*), and 0.5 mol L^{-1} (*5*); $[Q] = 0.2$ mol L^{-1}, $P(C_2H_4) = 0.87$ atm, $[Pd]_\Sigma = 0.0005$ mol L^{-1}, $\alpha(H_2O) = 0.67$ molar fractions.

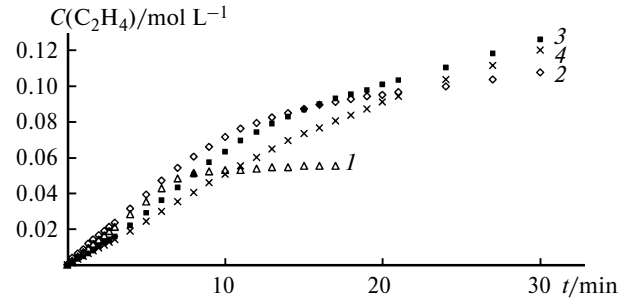

Fig. 3. Time dependences of the consumed ethylene concentration at various *p*-benzoquinone concentrations: $[Q] = 0.05$ (*1*), 0.1 (*2*), 0.2 (*3*), and 0.4 mol L^{-1} (*4*); $P(C_2H_4) = 0.87$ atm, $[Pd]_\Sigma = 0.0005$ mol L^{-1}, $[HClO_4] = 0.2$ mol L^{-1}, $\alpha(H_2O) = 0.67$ molar fractions.

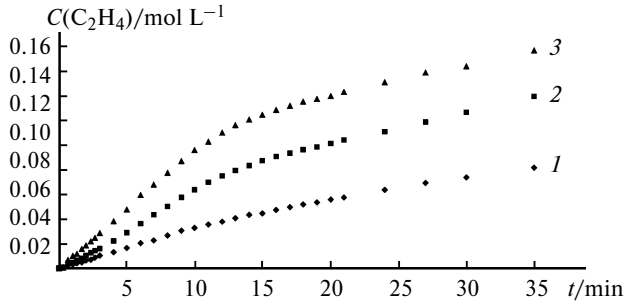

Fig. 4. Time dependences of the consumed ethylene concentration at various palladium concentrations: $[Pd]_\Sigma \cdot 10^4 = 2.5$ (*1*), 5 (*2*), 7.5 mol L^{-1} (*3*); $[Q] = 0.2$ mol L^{-1}, $P(C_2H_4) = 0.87$ atm, $[HClO_4] = 0.2$ mol L^{-1}, $\alpha(H_2O) = 0.67$ molar fractions.

Results and Discussion

To describe the process on time, the mechanism of ethylene oxidation (steps (1)—(10)) used for obtaining the kinetic equation of the reaction by the initial rates[15] was

supplemented by seven steps (steps (11)—(17)) that take into account the formation of the Pd^I complexes during the process and the appearance of the route (catalytic cycle) involving these complexes. The hypothesis of the mechanism of ethylene oxidation (see steps (1)—(17)) is based on the results of studying the reactivity of the cationic palladium complexes in an acetonitrile—water system. These results include the kinetics of the oxidation of cyclohexene by *p*-benzoquinone,[9] electronic absorption spectra of a $Pd(OAc)_2$—$HClO_4$—AN—H_2O system,[21] the KIE values in AN—H_2O/D_2O (see Ref. 11) and C_2H_4/C_2D_4 systems,[12] and determination of the shape of the kinetic dependences $R_0 = f(P(C_2H_4), [H^+], [Pd]_\Sigma, [Q])$.[15] In addition, the data of numerous experimental and theoretical studies on the kinetics and mechanism of olefin oxidation[22—24] and diverse oxidation reactions in solutions of the palladium complexes[25—27] were used.

$$Pd(AN)(H_2O)_3]^{2+} + C_2H_{4(s)} \rightleftharpoons$$
$$\rightleftharpoons [Pd(AN)(C_2H_4)(H_2O)_2]^{2+} \{\pi_1\} + H_2O \quad (1)$$

$$[Pd(AN)(C_2H_4)(H_2O_2)]^{2+} \{\pi_1\} \xrightarrow{H_2O}$$
$$\longrightarrow [Pd(AN)(CH_2CH_2O^+H_2)(H_2O)_2]^+ \{\sigma_1\} \quad (2)$$

$$[Pd(AN)(CH_2CH_2O^+H_2)(H_2O)_2]^+ \{\sigma_1\} \xrightarrow{H_2O}$$
$$\longrightarrow [Pd(AN)(CH_2CH_2OH)(H_2O)_2]^+ \{\sigma_2\} + H_3O^+ \quad (3)$$

$$[Pd(AN)(CH_2CH_2OH)(H_2O)_2]^+ \{\sigma_2\} \xrightarrow{H_2O}$$
$$\longrightarrow [Pd(AN)(H_2O)_2]^0 \{Pd^0\} + CH_3CHO + H_3O^+ \quad (4)$$

$$[Pd(AN)(H_2O)_2]^0 \{Pd^0\} + Q \rightleftharpoons$$
$$\rightleftharpoons [Pd(AN)(Q)]^0 \{PdQ^0\} + 2\,H_2O \quad (5)$$

$$[Pd(AN)(H_2O)_2]^0 \{Pd^0\} + 2\,Q \rightleftharpoons$$
$$\rightleftharpoons Pd(Q)_2{}^0 + AN + 2\,H_2O \quad (6)$$

$$[Pd(AN)(Q)]^0 \{PdQ^0\} + H_3O^+ \longrightarrow$$
$$\longrightarrow [Pd(AN)(OC_6H_4OH)(H_2O)]^+ \quad (7)$$

$$[Pd(AN)(OC_6H_4OH)(H_2O)]^+ \xrightarrow{+H_3O^+,\ H_2O}$$
$$\longrightarrow [Pd(AN)(H_2O)_3]^{2+} + QH_2 \quad (8)$$

$$[Pd(Q)_2]^0 + H_3O^+ + H_2O \rightleftharpoons$$
$$\rightleftharpoons [Pd(Q)(OC_6H_4OH)(H_2O)_2]^+ \{Pd(Q)(QH)^+\} \quad (9)$$

$$[Pd(Q)(OC_6H_4OH)(H_2O)_2]^+ \{Pd(Q)(QH)^+\} +$$
$$+ H_3O^+ \xrightarrow{+AN} [Pd(AN)(H_2O)_3]^{2+} + QH_2 + Q \quad (10)$$

$$[Pd(AN)(H_2O)_3]^{2+} + [Pd(AN)(H_2O)_2]^0 \rightleftharpoons$$
$$\rightleftharpoons [Pd_2(AN)_2(H_2O)_4]^{2+} + H_2O \quad (11)$$

$$[Pd_2(AN)_2(H_2O)_4]^{2+} + Q \longrightarrow$$
$$\longrightarrow [Pd_2(AN)_2Q(H_2O)_2]^{2+} + 2\,H_2O \quad (12)$$

$$[Pd_2(AN)_2Q(H_2O)_2]^{2+} + C_2H_{4(s)} \rightleftharpoons$$
$$\rightleftharpoons [Pd_2(AN)_2Q(C_2H_4)(H_2O)]^{2+} + H_2O \quad (13)$$

$$[Pd_2(AN)_2Q(C_2H_4)]^{2+} + H_2O \longrightarrow$$
$$\longrightarrow [Pd_2(AN)_2Q(CH_2CH_2O^+H_2)(H_2O)]^+ \{\sigma_3\} \quad (14)$$

$$[Pd_2(AN)_2Q(CH_2CH_2O^+H_2)(H_2O)]^+ \{\sigma_3\} \xrightarrow{H_2O}$$
$$\longrightarrow [Pd_2(AN)_2Q(CH_2CH_2OH)(H_2O)]^+ \{\sigma_4\} + H_3O^+ \quad (15)$$

$$[Pd_2(AN)_2Q(CH_2CH_2OH)(H_2O)]^+ \{\sigma_4\} + Q \longrightarrow$$
$$\longrightarrow [Pd_2(AN)_2Q(QH)(H_2O)]^+ + CH_3CHO \quad (16)$$

$$[Pd_2(AN)_2Q(QH)(H_2O)]^+ + H_3O^+ \longrightarrow$$
$$\longrightarrow [Pd_2(AN)_2Q(H_2O)_2]^{2+} + QH_2 \quad (17)$$

The brief designations of the intermediates are presented in braces for the steps of the mechanism for convenience of the further discussion (s implies solution).

It has previously been found[15] that the R_0 values increase with an increase in $[HClO_4]$ until almost constant values were achieved ("saturation" curve) and the KIE value[11] for the H_2O/D_2O pair is close to 1. These observations and facts assert that the system studied includes no step of water dissociation in the kinetically irreversible (slow) step (2) and in the preceding quasi-equilibrium steps. Therefore, the reaction of the π-complex with the water molecule (see step (2)) proceeds as the *anti*-addition of water from solution to ethylene, which is coordinated to the palladium cation with the formation of the palladiumcarbenium cation solvated by the water molecule (σ_1) (see also review[24]). It can be assumed that the redox decomposition of the intermediate (σ_1) to acetaldehyde and complex $[Pd(AN)(H_2O)_2]^0$ occurs after slow step (2) in fast irreversible steps (3) and (4). This assumption does not contradict the observation that the KIE value[12] for the C_2H_4/C_2D_4 pair is also close to 1. After stabilization of the Pd^0 complex by the reaction with *p*-benzoquinone in quasi-equilibrium steps (5) and (6), the second slow step occurs: oxidation of Pd^0 in the reaction with the acid

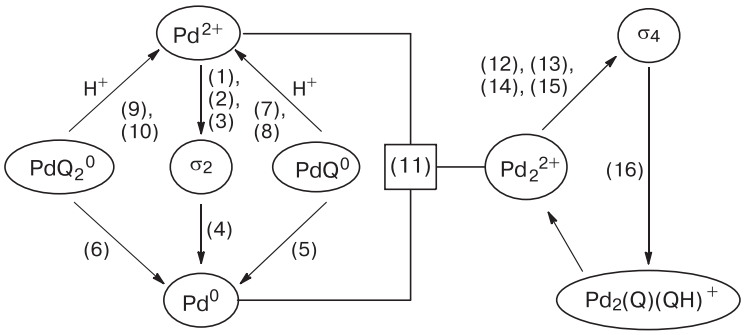

Fig. 5. Kinetic graph of the three-route mechanism of ethylene oxidation by *p*-benzoquinone with reversible nonlinear step (11).

(see step (7)), leading to the regeneration of the initial palladium(II) complex *via* the formation of palladium hydroquinolate. In a series of works[28,29] conducted in aqueous solutions, the type (7) step is considered as a rate-determining one. The Pd^0 complexes with quinones are well known,[30] as well as the oxidation of palladium(0) by *p*-benzoquinone in the presence of acids.[31,32] The step of oxidation of palladium(0) in the $Pd(Q)_2{}^0$ complex was included into the reaction mechanism for completeness of the model. Step (9) was regarded as quasi-equilibrium. We considered only one 1 : 1 π-complex of ethylene with Pd^{2+} in the proposed two-route scheme of the mechanism (see reactions (1)—(10)).[15]

The palladium(I) complex involved in the additional third route can be formed in reversible step (11). By analogy to step (3), step (14) is the formation of the intermediate organopalladium compound (σ_3) transformed in steps (15) and (16) *via* (σ_4) into acetaldehyde. Step (17) describes the regeneration of the complex formed at step (12).

The kinetic graph of mechanism (1)—(17) with one reversible nonlinear step (11), which clearly represents the mechanism structure and relationship of the routes, is shown in Fig. 5.

When writing the systems of differential equations for 17 steps of the assumed mechanism, it was taken into account that the concentrations of ethylene, acid, and acetonitrile (11.2 mol L^{-1}) remain unchanged in time. The water concentration (22.3 mol L^{-1}) remains nearly unaltered during the process. The equations of the law of mass action for the steps involving water or acetonitrile molecules include the overall concentrations of these components of the solvent. The rate constants of 17 steps and equilibria (six kinetically reversible steps) are presented in Table 1.

An analysis of identifiability of parameters of the model[33] showed eight unambiguous estimates of the parameters and parametric functions (PF): k_{12} (0.19), k_{16} (0.14), K_1k_2 (0.05), $k_6/(K_5k_7)$ (0.20), $K_{11}/(K_5k_7)$ (0.20), $k_5/(K_5k_7)$ (0.26), k_9k_{10} (0.31), and k_3k_4 (0.33) (logarithmic inaccuracies of the parameters and PF are given in parentheses).

Possible reasons for relations between the estimates of the constants and appearance of the PF are the following: quasi-equilibrium before the irreversible step (K_1k_2 and K_5k_7), quasi-stationarity (k_3k_4 and k_9k_{10}), and parallel (competitive) steps (k_5/k_6).

The examples of four of 14 calculated and experimental kinetic curves of the consumed ethylene concentration (or formed acetaldehyde concentration) are presented in Fig. 6.

An analysis of 14 kinetic curves of the consumed ethylene concentration under various conditions showed that a noticeable deviation of the calculated concentrations from the experimental ones in the second ("slow") region of the kinetic curve is observed only for four of them, and $C_{calc} > C_{exp}$ in the four cases. The root-mean-square error of the experiment description is 10.36%. Note that on the "fast" region of the curves the kinetic regularities are described by the initial rates[15] in terms of mechanism

Table 1. Rate (k_i) and equilibrium (K_i) constants for the steps of the ethylene oxidation mechanism

Step (*i*)	k_i	K_i
(1)	183.6	—
(2)	26.7	2.0
(3)	8.5	—
(4)	8.5	—
(5)	$2.7 \cdot 10^4$	1.95
(6)	$2.3 \cdot 10^4$	$1.0 \cdot 10^{10}$
(7)	$1.8 \cdot 10^8$	—
(8)	24.4	—
(9)	2.79	$2.9 \cdot 10^3$
(10)	5.49	—
(11)	$1.0 \cdot 10^{10}$	$3.1 \cdot 10^4$
(12)	250.0	—
(13)	$1.0 \cdot 10^{10}$	$1.0 \cdot 10^{10}$
(14)	5.25	—
(15)	5.55	—
(16)	21.8	—
(17)	$9.4 \cdot 10^6$	—

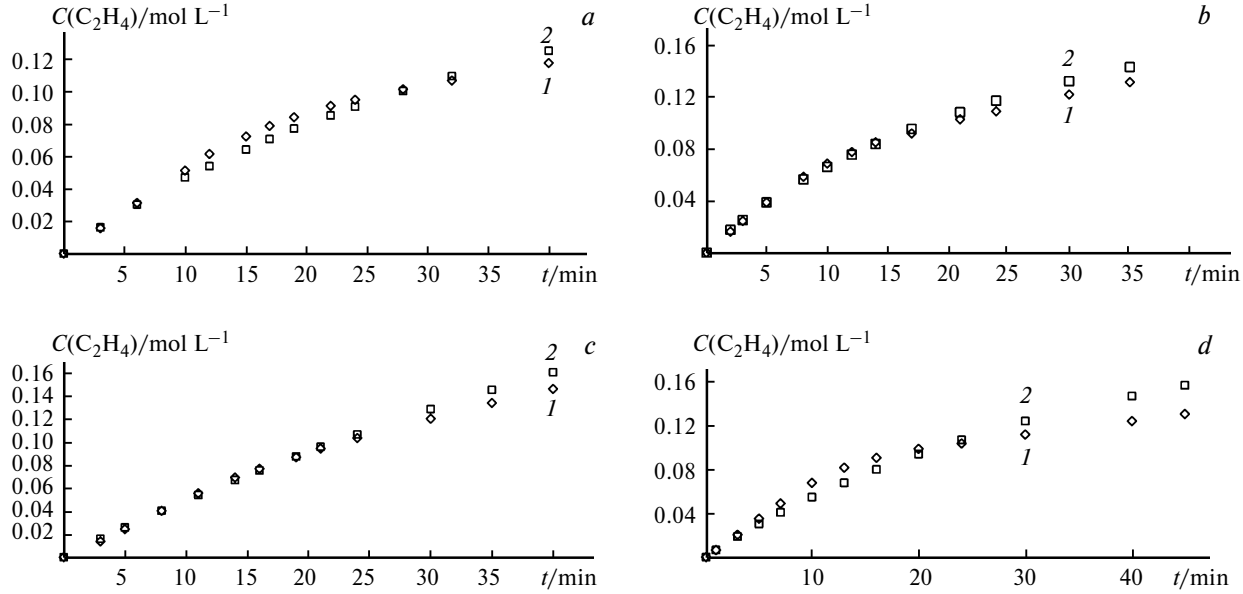

Fig. 6. Time dependences of the consumed ethylene concentration: *1*, experiment and *2*, calculation. Conditions: (*a*) [Q] = = 0.2 mol L^{-1}, $P(C_2H_4)$ = 0.6 atm, $[H^+]$ = 0.2 mol L^{-1}, $[Pd]_\Sigma = 5 \cdot 10^{-4}$ mol L^{-1}, $[LiClO_4]$ = 0.3 mol L^{-1}, α_{H_2O} = 0.67; (*b*) [Q] = 0.2 mol L^{-1}, $P(C_2H_4)$ = 0.87 atm, $[H^+]$ = 0.5 mol L^{-1}, $[Pd]_\Sigma = 5 \cdot 10^{-4}$ mol L^{-1}, α_{H_2O} = 0.67; (*c*) [Q] = 0.4 mol L^{-1}, $P(C_2H_4)$ = 0.87 atm, $[H^+]$ = 0.2 mol L^{-1}, $[Pd]_\Sigma = 5 \cdot 10^{-4}$ mol L^{-1}, $[LiClO_4]$ = 0.3 mol L^{-1}, α_{H_2O} = 0.67; (*d*) [Q] = 0.2 mol L^{-1}, $P(C_2H_4)$ = 0.87 atm, $[H^+]$ = 0.2 mol L^{-1}, $[Pd]_\Sigma = 5 \cdot 10^{-4}$ mol L^{-1}, $[LiClO_4]$ = 0.3 mol L^{-1}, α_{H_2O} = 0.67.

(1)—(10) with the root-mean-square error equal to 4.5%. A possible reason for description worsening can be an insufficiently substantiated choice of the composition of the coordination sphere of the palladium(II) and palladium(I) complexes in the intermediates of steps (1)—(17).

The material balance with respect to palladium ($[Pd]_\Sigma$ = = 0.0005 mol L^{-1}) during the process on regions **A** (1—15 min) and **B** (13—45 min) was analyzed taking into account the intermediates, whose concentration was >5 mol.% of $[Pd]_\Sigma$ (Table 2) for the following conditions: [Q] = 0.4 mol L^{-1}, $P(C_2H_4)$ = 0.87 atm (see Table 2, entry *1*, Fig. 6, *c*), [Q] = 0.2 mol L^{-1}, $P(C_2H_4)$ = 0.42 atm (entry *2*, see Fig. 1, curve *2*) and for the "standard" entry with [Q] = 0.2 mol L^{-1}, $P(C_2H_4)$ = 0.87 atm (entry *3*, see Fig. 6, *d*). A series of regularities can be revealed by the results of analysis of the material balance (mol.% Pd bound in σ_4 indicated in the tables taking into account two palladium atoms in σ_4).

A. Within 1—3 min the catalyst occurs mainly as Pd^{2+}, PdQ_2, and $PdQ(QH)^+$ or Pd^{2+}, PdQ_2, $PdQ(QH)^+$, and σ_4; Pd^{2+} and σ_4 or σ_4 at the end of the process (see Table 2).

B. The concentrations of all intermediates, except for σ_4, decrease in the course of the process, and palladium is accumulated in the form σ_4. A considerable accumulation of palladium in the form σ_4 is observed to the moment of completion of the fast region of the kinetic curves, *i.e.*, in 13—15 min.

C. The significant increase in the fraction of σ_4 to the end of the process is probably related to a lower ability of the organometallic σ-compound of Pd^I to the redox decomposition with acetaldehyde formation.

D. A decrease in the concentrations of *p*-benzoquinone [Q] from 0.4 mol L^{-1} (entry *1*) to 0.2 mol L^{-1} (entry *3*, see Table 2) decreases the concentrations of the intermediates PdQ_2, $PdQ(QH)^+$, and σ_4.

E. An increase in $P(C_2H_4)$ from 0.42 atm (entry *2*) to 0.87 atm (entry *3*) is accompanied by a decrease in the

Table 2. Distribution of $[Pd]_\Sigma$ (mol.%) in the intermediates

Time /min	$[Pd^{2+}]$	$[\sigma_1]$	$[\sigma_2]$	$[PdQ_2]$	$[PdQ(QH)^+]$	$[\sigma_4]$
$[Q]_0$ = 0.4 mol L^{-1}, $P(C_2H_4)$ = 0.87 atm (entry *1*)						
3	26.2	5.3	5.3	26.4	26.6	9.6
14	20.4	4.1	4.1	18.6	18.7	33.8
21	17.6	3.5	3.5	15.2	15.2	44.4
40	12.7	2.5	2.6	9.1	9.1	63.6
$[Q]_0$ = 0.2 mol L^{-1}, $P(C_2H_4)$ = 0.42 atm (entry *2*)						
3	45.6	—	—	13.0	13.1	17.7
15	27.4	—	—	6.4	6.4	53.6
22	21.8	—	—	4.5	4.6	64.0
40	14.1	—	—	2.2	2.2	78.4
$[Q]_0$ = 0.2 mol L^{-1}, $P(C_2H_4)$ = 0.87 atm (entry *3*)						
1	34.6	6.9	7.0	21.0	21.4	6.9
13	21.0	4.2	4.2	9.3	9.3	50.8
20	16.6	3.3	3.3	6.6	6.1	63.6
45	8.7	1.6	1.7	1.4	1.4	84.0

Table 3. Changes in the calculated rates for steps (4) and (16) of acetaldehyde formation on time

Entry	t/min	$W_4 \cdot 10^3$	$W_{16} \cdot 10^3$	$R_\Sigma \cdot 10^3$
		mol L^{-1} min^{-1}		
1	3	4.77	0.19	4.96
	14	3.69	0.60	4.29
	21	3.20	0.72	3.92
	40	2.3	0.89	3.19
2	3	4.0	0.176	4.17
	15	2.40	0.417	2.80
	22	1.92	0.437	2.36
	40	1.24	0.387	1.36
3	1	6.3	0.07	6.37
	3	5.7	0.18	5.88
	13	3.8	0.39	4.19
	20	3.0	0.41	3.41
	45	1.6	0.24	1.84

concentrations of Pd^{2+}, PdQ_2, and $PdQ(QH)^+$ and weakly affects the concentration of σ_4.

The following conclusions can be drawn from an analysis of changes in the rates of the steps of acetaldehyde formation (4) and (16) (Table 3) and the overall rate of the oxidation reaction R_Σ in time.

(1) Beginning from the first minute, the reaction rates of ethylene oxidation W_4 and R_Σ decrease as the Pd^{2+} concentrations decrease in reaction (11) (see Table 2) and Pd^{2+} is transformed into Pd_2^{2+} and further into σ_4.

(2) In the experiment with [Q] = 0.4 mol L^{-1} (see Table 3, entry *1*), the calculated (and experimental) rates of acetaldehyde formation change insignificantly with time until t = 21 min is achieved compared to entry *3* with [Q] = 0.2 mol L^{-1}. A weaker change in R_Σ within 40 min (1.5-fold decrease in the first case and 3.2-fold decrease in the second case) is also observed. These results are related, most likely, to the compensation of decreasing rate W_4 of step (4) (due to a decrease in $[Pd^{2+}]$) by an increase in the rate with a decrease in the quinone concentration in time on going from the initial quinone concentration equal to 0.4 mol L^{-1} to a concentration of 0.2 mol L^{-1}. This increase in the rate is accompanied by the experimentally found extremal dependence of the initial rate $R_0 = f([Q]_0)$,[15] which demonstrates an increase in the rate as the quinone concentration decreases from 0.4 to 0.2 mol L^{-1} (see rate values W_4 at t = 3 min in Table 3, entries *1* and *3*). The lower change in the reaction rate R_Σ in entry *1* is also affected by a substantial increase in the contribution of the third route (W_{16}) in R_Σ with time. For example, in the experiment with [Q] = 0.4 mol L^{-1} the contribution of third route to the overall rate at t = 40 min is 28%. In this case, the quinone concentration does not increase to an extremum ([Q] = 0.1 mol L^{-1}) even within 40 min at the 60% quinone conversion, while this extremum is attained within 13—15 min at the initial quinone concentration 0.2 mol L^{-1} (see Table 3, entry *3*).

(3) The rates of acetaldehyde formation *via* the third route (W_{16}) pass through small maxima with time (see Table 3, entries *2* and *3*). In entry *1*, the maximum of W_{16} is not attained within 40 min.

(4) At the maximum values of the rate W_{16}, the contribution of the third route to the overall reaction rate is 28, 18, and 12% in entries *1*, *2*, and *3*, respectively.

(5) A comparison of entries *2* and *3* shows that a twofold increase in $P(C_2H_4)$ regularly results in an increase in the rate W_4 at all steps of the process.

(6) It is most likely that the rates of steps (16) and (17) are insufficiently high for the fast regeneration of the catalytically active palladium(I) complex $[Pd_2(AN)_2Q(H_2O)_2]^{2+}$ formed in step (12).

Thus, in the first "fast" region of the kinetic curve (**A**), the initial concentration of the cationic Pd^{2+} complex rapidly decreases (by 70—80%), since only 20—27% of the taken palladium remain in the system. The third route appears with the Pd^I complexes and accumulation of σ_4 containing 30—50% total palladium. This intermediate is the major one in the third route. A noticeable contribution of the third route is observed only at a high quinone concentration (0.4 mol L^{-1}). A higher rate of decomposition of σ_4 to acetaldehyde also takes place only at an elevated concentration of Q due to its assumed participation in step (16). The maximum of the reaction rate with respect to [Q] (see Ref. 15) is explained by an appreciable binding of palladium into the PdQ_2 complex (see constant K_6 in Table 1) and the corresponding decrease in the concentration of active Pd^{2+} (see Table 2, $[Pd^{2+}]$ and $[PdQ_2]$). In the slow region of the kinetic curve (**B**), a continuous increase in the concentration of σ_4 is observed within a continuous decrease in the concentrations of all intermediates and quinone (<0.1 mol L^{-1}, entry *3*), whereby the W_4 rate also decreases.

Since the possibility of catalysis of ethylene oxidation by the $[Pd(Q)]^0$ and $[Pd(C_2H_4)(Q)]^0$ complexes has previously been assumed[28,29] for aqueous solutions of the cationic palladium complexes, we additionally considered the fourth route including steps (18)—(23).

$$[Pd(AN)(H_2O)_2]^0 + 2\ C_2H_{4(s)} \rightleftharpoons \rightleftharpoons [Pd(AN)(C_2H_4)_2]^0 + 2\ H_2O \quad (18)$$

$$[Pd(AN)(Q)]^0 + 2\ C_2H_{4(s)} \rightleftharpoons \rightleftharpoons [Pd(C_2H_4)(Q)]^0 + AN \quad (19)$$

$$[Pd(C_2H_4)(Q)]^0 + H_3O^+ \longrightarrow \longrightarrow [Pd(C_2H_4)(QH)(H_2O)]^+ \quad (20)$$

$$[Pd(C_2H_4)(QH)(H_2O)]^+ + H_2O \longrightarrow \longrightarrow [Pd(C_2H_4O^+H_2)(QH)(H_2O)]^0 \quad (21)$$

$$[Pd(C_2H_4O^+H_2)(QH)(H_2O)]^0 + H_2O \longrightarrow$$
$$\longrightarrow [Pd(C_2H_4OH)(QH)(H_2O)]^0 + H_3O^+ \quad (22)$$

$$[Pd(C_2H_4OH)(QH)(H_2O)]^0 + AN + H_2O$$
$$\longrightarrow [Pd(AN)(H_2O)_2]^0 + QH_2 + CH_3CHO \quad (23)$$

This route is interesting by the fact that the oxidation of complex $[Pd(C_2H_4)(Q)]^0$ in the reaction with H_3O^+ immediately results in the hydroquinolate π-Pd^{II} complex, which further interacts with the water molecule. However, an analysis showed that the quality of description was not practically improved (error 10.26%).

The description of the mechanism can further be improved using additional data on the coordination spheres of all intermediates of the mechanism. This information can be provided by quantum chemical study. In this work, we calculated the Gibbs energies of steps (1), (4), (5), (11), and (12) in order to refine the composition of the coordination sphere of palladium in the key intermediates of the mechanism: $[Pd(\pi\text{-}C_2H_4)(AN)(H_2O)_2]^{2+}$, $[Pd(AN)(H_2O)_2(\sigma\text{-}C_2H_4O^+H_2)]^+$, $[Pd(AN)_x(H_2O)_y]^0$, and $[Pd_2Q(AN)_4]^{2+}$. In addition, for the further development of the theory of mechanisms of oxidation reactions involving the π-palladium complexes, it is important to obtain an additional information about probable mechanisms of the steps of the reactions of the π-palladium complexes with the nucleophiles (H_2O) and steps of deprotonation of the formed intermediates. To approach the problem, we estimated the activation barriers of steps (2) and (3) of the mechanism.

Step (1). The displacement of the water or acetylene molecule is possible in the step of ethylene addition to the $[Pd(AN)(H_2O)_3]^{2+}$ complex. The modeling of this step taking into account two perchlorate ions solvated by two water molecules and one AN molecule resulted in the Gibbs energies $\Delta G_{298} = -4.3$ and -2.2 kcal mol^{-1} for reactions (1.1) and (1.2), respectively. Thus, when the formation of the coordination complex involves ethylene, the displacement of the water molecule (1.1) is the energetically favorable process.

$$[Pd(AN)(H_2O)_3]^{2+} + C_2H_4 \rightleftharpoons$$
$$\rightleftharpoons [Pd(\pi\text{-}C_2H_4)(AN)(H_2O)_2]^{2+} + H_2O \quad (1.1)$$

$$[Pd(AN)(H_2O)_3]^{2+} + C_2H_4 \rightleftharpoons$$
$$\rightleftharpoons [Pd(\pi\text{-}C_2H_4)(H_2O)_3]^{2+} + AN \quad (1.2)$$

The absence of counterions for modeling step (1) leads to an energetically unfavorable relative to $Pd(AN)_2{}^0$ reaction. For example, for reaction (1.2) ΔG_{298} becomes equal to 16.8 kcal mol^{-1}.

Steps (2) and (3). Since an analysis of the potential energy surface (PES) of these steps is difficult, we first considered the systems in the absence of solvated perchlorate anions. Modeling of the nucleophilic attack of the π-palladium complex by a single water molecule results in the barrier-free formation of the $[Pd(AN)(H_2O)_2(\sigma\text{-}C_2H_4O^+H_2)]^+$ complex (step (2)), but the product of deprotonation of this complex in step (3) has no minimum on the PES and the second water molecule is simply bound to the first H_2O molecule by the hydrogen bond. Only the addition of the third water molecule leads to deprotonation. Therefore, step (3) can be written as follows:

$$[Pd(AN)(H_2O)_2(\sigma\text{-}C_2H_4O^+H_2)]^+ + 2\ H_2O \longrightarrow$$
$$\longrightarrow [Pd(AN)(H_2O)_2(\sigma\text{-}C_2H_4OH)]^+ + H_5O_2{}^+. \quad (3.1)$$

It is known (see review in the book,[27] chapter 8) that the addition of organic polar solvents to water in an amount of 0.3 molar fraction decomposes the tetrahedral three-dimensional network of water and results in the formation of small associates $(H_2O)_n$. Therefore, an assumption about the participation of water associates in elementary steps of the mechanisms can be considered as valid. In addition, the kinetic experiments described above were carried out at the molar fraction of acetonitrile equal to 0.33. Hence, additional calculations of step (2) were performed using an associate of three water molecules (trimer).

The calculations showed that the addition of the water trimer to ethylene in the π-complex requires no activation energy and can lead to two different products. In the case of the attack of ethylene in the π-complex by the oxygen atom of the terminal water molecule of the trimer (as in Ref. 34), the addition of the trimer is accompanied by the deprotonation and displacement of $H_5O_2{}^+$ from the latter. The product identical to the product of step (3.1) is formed in this elementary step (3.2) (see Fig. 7, *a*).

$$[Pd(AN)(H_2O)_2(\pi\text{-}C_2H_4)]^{2+} + (H_2O)_3 \longrightarrow$$
$$\longrightarrow [Pd(AN)(H_2O)_2(\sigma\text{-}C_2H_4OH)]^+ + H_5O_2{}^+ \quad (3.2)$$

In the case where the central water molecule of the trimer is an attacker, the formation of the product (Fig. 7, *b*) is not accompanied by the rejection of a proton or water molecules into the external sphere (step (2.1)).

$$[Pd(AN)(H_2O)_2(\pi\text{-}C_2H_4)]^{2+} + (H_2O)_3 \longrightarrow$$
$$\longrightarrow [Pd(AN)(H_2O)_2(\sigma\text{-}C_2H_4O^+H_2(H_2O)_2)]^+ \quad (2.1)$$

The deprotonation of the $\{Pd(AN)(H_2O)_2[\sigma\text{-}C_2H_4O^+H_2(H_2O)_2]\}^+$ complex (see Fig. 7, *b*) becomes possible due to the rearrangement related to the turn of the $CH_2O^+H_2(H_2O)_2$ fragment about the C—C bond from the *anti*- to *syn*-position with the formation of the Pd—O bond and rejection of the *cis*-coordinated water molecule and the water molecule from the associate to the external sphere of the complex together with the proton. The

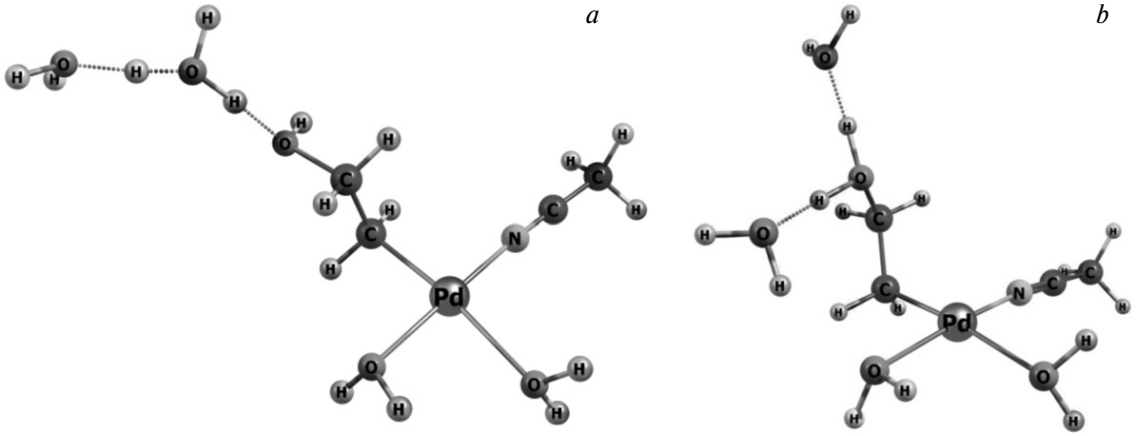

Fig. 7. Optimized structures of the products of steps (3.2) (*a*) and (2.1) (*b*).

product of step (3.3) of the transformation of complex $[Pd(AN)(H_2O)_2(\sigma\text{-}C_2H_4O^+H_2(H_2O)_2)]^+$ is presented in Fig. 8.

The formation of a similar palladacycle has been considered earlier[23,35] in the case of the palladium chloride complexes for the *cis*-insertion of ethylene into the Pd—OH bond, which occurs synchronously with the deprotonation of the product of H_2O molecule addition to ethylene in the π-complex. Step (3.3) unifies the step of formation of the $[Pd(AN)(H_2O)\{\sigma,\sigma\text{-}C_2H_4OH(H_2O)\}...\{H_5O_2\}]^+$ complex (see Fig. 8) from the product of step (2.1) (see Fig. 7, *b*) and the step of $H_5O_2^+$ ion transfer from the external sphere of the complex to the solution.

$$[Pd(AN)(H_2O)_2(\sigma\text{-}C_2H_4O^+H_2(H_2O)_2)]^+ \longrightarrow$$

$$\longrightarrow [Pd(AN)(H_2O)\{\sigma,\sigma\text{-}C_2H_4OH(H_2O)\}]^+ + H_5O_2^+ \quad (3.3)$$

According to the calculations, the Gibbs activation energy of step (3.3) is 7.4 kcal mol^{-1}.

At the next stage, we performed modeling of steps (2) and (3) taking into account counterions. Note that the amount of water molecules solvating perchlorate ions defines how close to palladium atoms in the π-complex can approach the perchlorate ions. If each anion is solvated by one, two, or six water molecules, then the Pd—Cl distance (Cl in ClO_4^-) in the ion pair on the average is equal to 4.4, 4.6, or 6.3 Å, respectively. The further calculations were performed in the model with perchlorate ions solvated by six water molecules.

When considering step (2), the addition of perchlorate ions mainly leads to two effects, The first effect is associated with the appearance of an insignificant activation barrier of 3.6 kcal mol^{-1}. The second effect is related to structural changes: the proton moves from the oxygen atom of the palladoethanol fragment (Fig. 9) at a longer distance (5.1 Å) compared to that in the product of step (3.2) (3.1 Å). The presence of hydrated anions leads essentially to the elimination of the water molecule from the solvation network for the addition to the π-complex with the appearance of an insignificant activation barrier of 3.6 kcal mol^{-1}, but the addition product is simultaneously deprotonated to form the palladoethanol complex due to the chain of hydrogen bonds. Probably, these two processes result in the appearance of a low barrier. A similar effect was observed for the attack of the π-complex by the terminal water molecule of the trimer.

When analyzing the steps of type (2) and others in which the associated solvent molecule (H_2O, ROH, RCOOH, PhOH, ROOH) is the reactant, a natural question arises: how the concentration of the free molecule, for example, H_2O, or of the needed associate for example, $(H_2O)_n$, can be expressed in the kinetic equation? The concentration of the associate molecule $(H_2O)_3$ can be expressed through $[H_2O]_\Sigma$ if the type of the dependence of the free water molecule concentration on its overall concentration is known: $[H_2O] = f([H_2O]_\Sigma)$. The approaches to the solution of similar problems related to the formation of associates or polynuclear metal complexes are presented in the monograph[27] (chapter 2).

Step (4). The complexes of various compositions $[Pd(AN)_x(H_2O)_y]^0$ were calculated to reveal the most

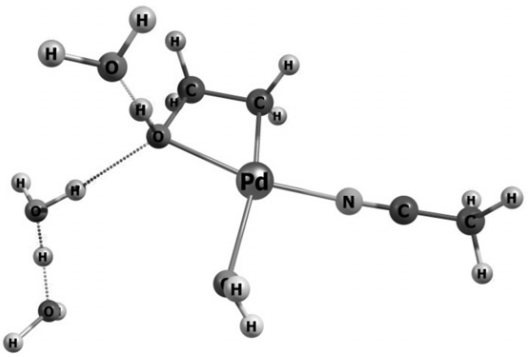

Fig. 8. Structure of complex $[Pd(AN)(H_2O)\{\sigma,\sigma\text{-}C_2H_4OH(H_2O)\}...\{H_5O_2\}]^+$.

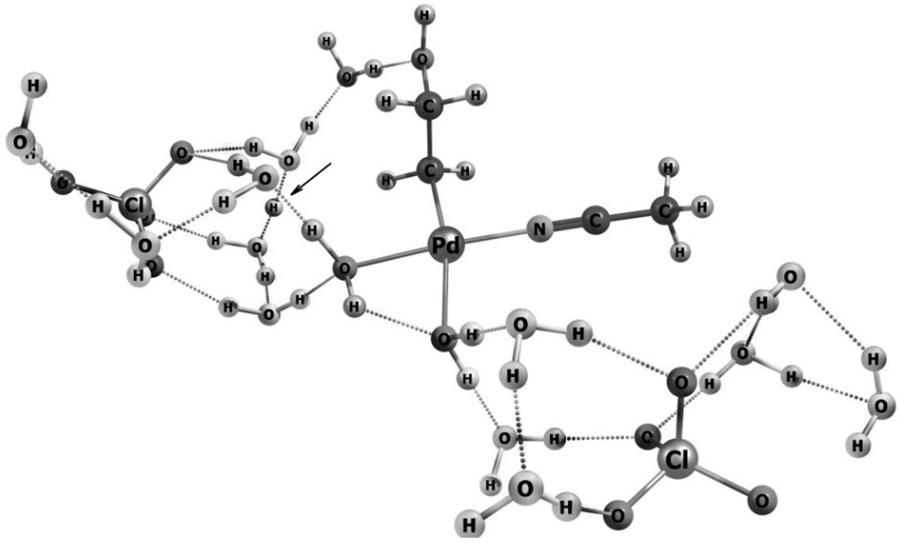

Fig. 9. Structure of complex $[Pd(AN)(H_2O)_2\{\sigma\text{-}C_2H_4OH(H_2O)\}][ClO_4\{H_2O\}_6]...\{H_5O_2\}^+$ $[ClO_4\{H_2O\}_4]^-$. The water molecules forming the solvate shell of perchlorate ions marked with light background. The proton in the $\{H_5O_2\}^+$ form is indicated by arrow.

probable composition of the Pd^0 complexes formed in step (4). According to the calculations, the dinitrile complex $Pd(AN)_2{}^0$ is characterized by the highest energy stability. The tetrahedral ($Pd(AN)_4{}^0$) and planar ($Pd(AN)_3{}^0$) complexes having minima on the PES are thermodynamically unfavorable (by 23.9 and 11.8 kcal mol^{-1}, respectively). The replacement of the AN molecule by H_2O in $Pd(AN)_2{}^0$ with the formation of the two-ligand complex $[Pd(AN)(H_2O)]^0$ results in an 11.5 kcal mol^{-1} increase in the Gibbs energy.

Step (5). The addition of the *p*-benzoquinone molecule (Q) to $Pd(AN)_2{}^0$ *via* the η^2-type is very favorable ($\Delta G_{298} = -13.8$ kcal mol^{-1}) and proceeds exothermically ($\Delta H_{298} = -25.0$ kcal mol^{-1}). The addition of the second Q molecule that proceeds with the displacement of the AN ligand is also favorable ($\Delta G_{298} = -7.2$ kcal mol^{-1}).

Step (11). The reaction of the Pd^{II} and Pd^0 complexes is thermodynamically favorable and occurs without a barrier:

$$[Pd(AN)(H_2O)_3]^{2+} + Pd(AN)_2 \rightleftharpoons \rightleftharpoons [Pd_2(AN)_3(H_2O)_2]^{2+} + H_2O. \quad (11.1)$$

At the next step, the binuclear Pd^I complex can built up the coordination sphere without a barrier:

$$[Pd_2(AN)_3(H_2O)_2]^{2+} + AN \rightleftharpoons \rightleftharpoons [Pd_2(AN)_4(H_2O)_2]^{2+} \quad (11.2)$$

or

$$[Pd_2(AN)_3(H_2O)_2]^{2+} + H_2O \rightleftharpoons \rightleftharpoons [Pd_2(AN)_3(H_2O)_3]^{2+}. \quad (11.3)$$

The variant with AN (11.2) is energetically more favorable (gain of 10.5 kcal mol^{-1} in the absence of counterions and 3.8 kcal mol^{-1} in the presence of 2 $[(ClO_4)(H_2O)_6]^-$).

Step (12). A molecule of Q can be coordinated to the Pd^I complexes *via* the mono- or bidentate mode. The

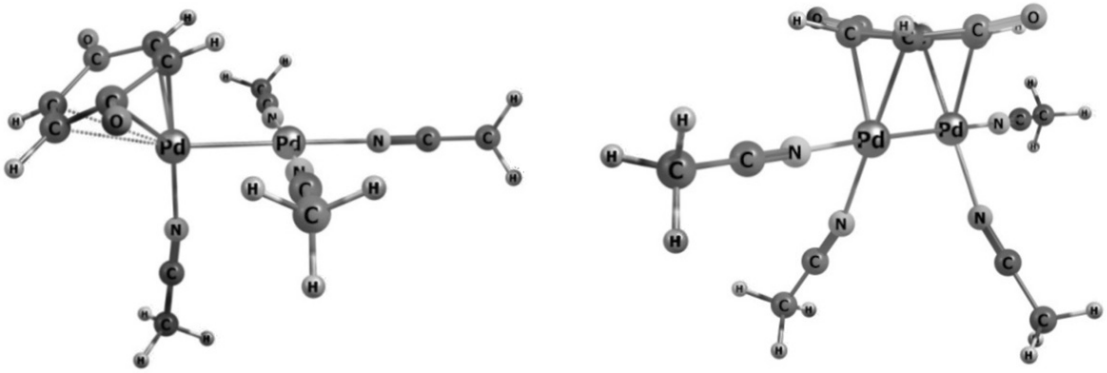

Fig. 10. Optimized structures of complex $[Pd_2(\eta^4\text{-}Q)(AN)_4]^{2+}$.

second variant is energetically more preferable (gain of 3.0 kcal mol^{-1} in the absence of counterions and 5.7 kcal mol^{-1} in the presence of 2 $[(ClO_4)(H_2O)_6]^-$). It can be assumed that the water molecules from the primary adduct $[Pd_2(AN)_3(H_2O)_3]^{2+}$ or $[Pd_2(AN)_4(H_2O)_2]^{2+}$ upon interacting with Q would leave the coordination sphere of the binuclear complex as "weak" ligands and finally the Pd^I complex $[Pd_2Q(AN)_4]^{2+}$ would be formed. The Q molecule can be either terminal (nearly η^4-coordination) or central with η^4-coordination (Fig. 10).

It was found by the performed preliminary calculations of the energy characteristics of several intermediates and steps that only the composition of the π-complex corresponds to the oxidation mechanism accepted for description (step (1)). The most probable compositions of the coordination spheres of the complexes have changed: that of the palladium(0) complex in step (4) $Pd(AN)_2^0$, palladium(I) in step (11) $[Pd_2(AN)_4(H_2O)_2]^{2+}$, and in step (12) $[Pd_2(\eta^4\text{-}Q)(AN)_4]^{2+}$. New versions appeared for the steps of H_2O addition to the π-complex (step (2)) and deprotonation of the obtained organometallic σ-compound (step (3)) involving of associates of water molecules. Evidently, the quantum chemical simulation of all other steps of the mechanism ((1)—(17)) in the AN—H_2O system should be performed in future and an improved mechanism should be used for analysis of the kinetic data after the preliminary solution of the problem of expressing concentrations of the associates through the overall water concentration.

This work was financially supported by the Russian Science Foundation (G. E. Efremov, Project No. 16-19-10632).

References

1. A. Sen, Lai Ta-Wang, *J. Am. Chem. Soc.*, 1981, **103**, 4627.
2. A. Sen, Lai Ta-Wang, *Organometallics*, 1982, **1**, 415.
3. Lai Ta-Wang, A. Sen, *Organometallics*, 1984, **3**, 866.
4. L. S. Hegedus, T. A. Mulbern, H. Asada, J. *Am. Chem. Soc.*, 1986, **108**, 6224.
5. J. Tsuji, M. Minato, *Tetrahedron Lett.*, 1987, **28**, 3683.
6. J.-E. Bäckvall, R. B. Hopkins, *Tetrahedron Lett.*, 1988, **29**, 2885.
7. D. G. Miller, D. D. M. Wayner, *J. Org. Chem.*, 1990, **55**, 2924.
8. M. Scumov, E. Balbolov, *Catal. Lett.*, 2000, **69**, 103.
9. O. N. Temkin, L. G. Bruk, D. S. Zakharova, K. Yu. Odintsov, E. A. Katsman, I. V. Petrov, O. Yu. Istomina, *Kinet. Catal.*, 2010, **51**, 691.
10. D. S. Zakharova, A. N. Semenyako, O. A. Chertkova, A. V. Frolkova, E. A. Katsman, L. G. Bruk, O. N. Temkin, *Tonkie Khim. Tekhnol.* [*Fine Chemical Technologies*], 2015, **10**, 77 (in Russian).
11. O. N. Temkin, D. S. Zakharova, O. A. Chertkova, A. S. Chelkin, L. G. Bruk, *Russ. Chem. Bull.*, 2013, **62**, 844.
12. I. V. Martynov, G. E. Efremov, O. N. Temkin, *Russ. Chem. Bull.*, 2017, **66**, 922.
13. B. J. Anderson, J. A. Keith, M. S. Sigman, *J. Am. Chem. Soc.*, 2010, **132**, 11872.
14. G. E. Efremov, E. A. Bovyrina, A. V. Podtyagina, I. V. Oshanina, O. N. Temkin, *Kinet. Catal.*, 2019, **60**, 52.
15. I. V. Martynov, G. E. Efremov, E. A. Bovyrina, E. A. Katsman, O. N. Temkin, *Kinet. Catal.*, 2018, **59**, 436.
16. D. N. Laikov, *Chem. Phys. Lett.*, 1997, **281**, 151.
17. D. N. Laikov, Yu. A. Ustynyuk, *Russ. Chem. Bull.*, 2005, **54**, 820.
18. J. P. Perdew, K. Burke, M. Ernzerhof, *Phys. Rev. Lett.*, 1996, **77**, 3865.
19. D. N. Laikov, *Chem. Phys. Lett.*, 2005, **416**, 116.
20. E. A. Katsman, A. S. Berenblyum, *Paket programm dlya postroeniya i analiza kineticheskikh modelei i ego primenenie*, *MITKhT im. M. V. Lomonosova* [*Program Software for Construction and Analysis of Kinetic Models and Its Application, M. V. Lomonosov Moscow Institute of Fine Chemical Technologies*], Moscow, 2010 (in Russian).
21. D. S. Zakharova, I. V. Martynov, V. M. Nosova, O. N. Temkin, *Tonkie Khim. Tekhnol.* [*Fine Chemical Technologies*], 2016, **11**, No. 2, 57 (in Russian).
22. I. I. Moiseev, *π-Kompleksy olefinov v zhidkofaznom okislenii* [*π-Complexes of Olefins in Liquid-Phase Oxidation*], Nauka, Moscow, 1970, 270 pp. (in Russian).
23. J. A. Keith, P. M. Henry, *Angew. Chem., Int. Ed.*, 2009, **48**, 9038.
24. O. N. Temkin, *Kinet. Catal.,* 2014, **55**, 172.
25. O. N. Temkin, L. G. Bruk, *Oxidative Carbonylation — Homogeneous. Encyclopedia of Catalysis*, Ed. I. T. Horvath, Wiley-Interscience, Hoboken, New Jersey, 2003, V. **5**, 394 pp.
26. O. N. Temkin, L. G. Bruk, *Kinet. Katal.*, 2003, **44**, 661 [*Kinet. Catal.* (*Engl. Transl.*), 2003, **44**].
27. O. N. Temkin, *Homogeneous Catalysis with Metal Complexes. Kinetic Aspects and Mechanisms*, Wiley, Chichester, UK, 2012.
28. K. I. Matveev, N. B. Shitova, E. G. Zhizhina, *Kinet. Katal.*, 1976, **17**, 893 [*Kinet. Catal.* (*Engl. Transl.*), 1976, **17**].
29. E. G. Zhizhina, N. B. Shitova, K. I. Matveev, *Kinet. Katal.*, 1981, **22**, 1451 [*Kinet. Catal.* (*Engl. Transl.*), 1981, **22**].
30. A. V. Kulik, L. G. Bruk, O. N. Temkin, V. R. Khabibulin, V. K. Belsky, V. E. Zavadnik, *Mendeleev Commun.*, 2002, **12**, 47.
31. H. Grennberg, A. Gogoll, J.-E. Bäckvall, *Organometallics.*, 1993, **12**, 1790.
32. B. V. Popp, S. S. Stahl, *Top Organomet. Chem.*, 2007, **22**, 149.
33. V. G. Gorskii, E. A. Katsman, F. D. Klebanova, A. A. Grigor´ev, *Teor. Eksp. Chem.*, 1987, **23**, 181.
34. P. E. M. Siegbahn, *J. Phys. Chem.*, 1996, **100**, 14672.
35. J. A. Keith, R. J. Nielsen, J. Oxgaard, W. A. Goddard, *J. Am. Chem. Soc.*, 2007, **129**, 12342.

Received November 15, 2018;
in revised form March 18, 2019;
accepted April 4, 2019